Dynamics of coherent optical phonon generation and decay in GaP

B. K. Rhee* and W. E. Bron†
Department of Physics, Indiana University, Bloomington, Indiana 47405
(Received 16 June 1986)

Coherent longitudinal optical (LO) phonons are generated through nonlinear excitation by laser light. It is observed that the vibronic sideband structure associated with coherent LO phonons, and that of the acoustic phonons, generated during the dephasing of the LO phonons have an unexpected dependence on the power of the excitation lasers. The effect is traced to the presence of an electron-hole plasma which is shown to influence the phonon generation process. Moreover, it is directly verified that the dephasing of coherent near-zone-center longitudinal optical phonons in GaP is dominated by anharmonic decay into two half-energy longitudinal acoustic phonons.

I. INTRODUCTION

We report on an investigation of processes involved in the generation and decay of coherent, near-zone-center, longitudinal optical (LO) phonons (with frequency ω_{LO} and wave vector $q\sim 0$). Nonlinear mixing of picosecond pulses from dual synchronously pumped dye lasers has been previously reported to produce coherent LO phonons in GaP through coherent Raman excitation (CRE).[1,2] Subsequent phonon dephasing was observed, directly in the time domain, through measurements of the temporal evolution of the intensity of a time-resolved coherent anti-Stokes Raman scattering (TRCARS) signal. It was postulated, in the case of GaP, that at low temperatures, dephasing proceeds solely through anharmonic decay to produce longitudinal acoustic (LA) phonons such that

$$\mathrm{LO}(\omega_{\mathrm{LO}},0)\rightleftarrows \mathrm{LA}(\omega_{\mathrm{LO}}/2,q)+\mathrm{LA}(\omega_{\mathrm{LO}}/2,-q)\ .$$

In the present paper we first demonstrate experimentally that this is in fact so.[3] Moreover, we observe for the first time that the formation of coherent LO phonons can be strongly influenced by a nonlinear polarization associated with the presence of an electron-hole plasma generated by an excitation of carriers through two-photon absorption. These findings add another facet to the evolving picture of the interaction of optical phonons with various short-lived electronic excitations in semiconductors.[4]

Unfortunately, the LA phonon produced through the decay of the coherent LO phonons are not Raman active and can, accordingly, not be observed by the TRCARS technique. Instead we determine the frequency distribution of the LA and LO phonons through vibronic sideband phonon spectroscopy (VSPS).[5] In this method the vibronic interaction between the phonons and an impurity based luminescent state is used to produce phonon sidebands. In the present work the luminescence is associated with the decay of bound excitons.[6] Note that with the solid held at liquid helium temperatures, the only observable contribution to the anti-Stokes vibronic sideband result from the presence of nonequilibrium phonons.

II. EXPERIMENTAL TECHNIQUES AND RESULTS

As in the case of coherent Raman excitation with picosecond duration laser pulses,[1,2] two synchronously pumped dye laser pulse trains are required to produce coherent excitation of LO phonons in GaP. However, in the present case, the strength of the vibronic sideband signal is orders of magnitude weaker than that of the CARS signal. Hence, laser excitation with higher-energy pulses are required. Accordingly, a nitrogen laser was used with pulses of 5-ns duration, peak power of 400 KW, and with variable repetition rate of from 1 to 50 Hz. The laser output beam is split to synchronously pump two identical (Coumarin) dye lasers which were constructed following the design by Hanna *et al.*[7] The maximum energy per pulse of each dye laser is about 50 μJ with a duration of 5 ns and a spectral width of 5 ± 1 cm^{-1}. Parallel beams, one from each dye laser, are focused and overlapped inside the GaP sample with a 120-mm focusing lens. The luminescence is collected at 90°, analyzed with a 1-m Czerny-Turner spectrometer and recovered through a fast photomultiplier and is then preamplified and followed by Boxcar averaging. In order to observe useful signals it is necessary to increase the spectrometer slit width to ~ 300 μm, i.e., to a Gaussian instrumental halfwidth of ~ 9 cm^{-1}.

A single crystal of GaP was used with an estimated[8] nitrogen impurity concentration of $\sim 5.8\times 10^{16}$ cm^{-3}. Four sides of the crystal are polished to produce a sample of 4 mm$\times$4 mm$\times$7 mm in dimension. The sample is held in vacuum with one face in direct contact with the cold finger of a liquid-helium cryostate. One dye laser is operated at a frequency of $\omega_l = 18\,725$ cm^{-1}, which together with the other laser operated at $\omega_s = 18\,322$ cm^{-1}, makes up the difference frequency $\omega_{\mathrm{LO}}=\omega_l-\omega_s=403$ cm^{-1} required for nonlinear excitation of $q\sim 0$ coherent LO phonons in GaP. The maximum energy per laser pulse of ~ 50 μJ results[8] in an initial LO phonon concentration $n_{\mathrm{LO}}=5\times 10^{16}$ cm^{-3}, located within the overlap volume of the two laser beams.

The laser operating at ω_l also serves to excite the luminescence from the bound exciton in GaP[6] (zero phonon line at 18 688 cm^{-1}) with which the vibronic sidebands are associated. The resultant anti-Stokes vibronic sidebands are shown in Fig. 1. The hatched area covers the frequency range obscured by the tail of the l laser. The remainder shows quite clearly an increase in the sideband intensity at $\omega_{\mathrm{LO}}=403$ cm^{-1} and at $\omega_{\mathrm{LO}}/2=201.5$ cm^{-1}. No other phonon peaks are observed during an ef-

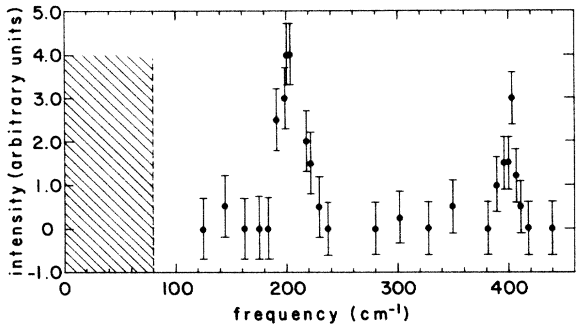

FIG. 1. Anti-Stokes vibronic sideband intensity as a function of phonon frequency. Spectral resolution is 9 cm^{-1}.

fective observation time of about 5 ns governed by the transit time of LA phonons through the cross section of the laser overlap volume. Thus, to within present experimental conditions, we demonstrate that the dominant decay mode for LO phonons in GaP is indeed as previously postulated.

The results shown in Fig. 1 were obtained with the sample at about 4.2 K and the power of the s- and l-lasers being, respectively, 75 and 135 MW/cm^2. In Figs. 2(a) and 2(b) we present the observed dependence of the anti-Stokes sideband intensity as measured at the LO and the LA peak frequencies as a function of the power in the s-laser when the power of the l-laser is fixed at 135 MW/cm^2. We observe that the intensities of both the LO and LA peaks undergo a maximum value at the s-laser-peak power of approximately 75 MW/cm^2. The large uncertainties in the intensities shown in Fig. 1 and Fig. 2 stem from the weakness of the vibronic signal, photomultiplier noise, and drifts in the signal recovery system which makes long-time signal averaging difficult. Normal integration times for each data point was about 5 m.

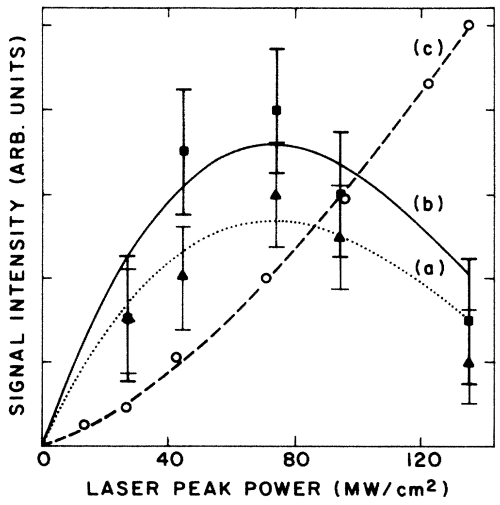

FIG. 2. Anti-Stokes vibronic sideband intensity as a function of s-laser peak power for (a) the LO peak, the LA peak, and (c) the 2-beam CARS signal intensity at $2\omega_l-\omega_s$. Symbols are experimental points and the solid, dashed, and dotted lines are theoretical fits to the data. The l-laser peak power is fixed at 135 MW/cm^2.

A final experimental observation was obtained by measuring a three-wave-mixing signal at the frequency $2\omega_l-\omega_s'$ with $\omega_l=18\,725$ cm^{-1} and $\omega_s'=18\,522$ cm^{-1}. The nonlinear response of GaP under these conditions is similar to those involved in CRE of optical phonons, but since $\omega_l-\omega_s'$ is not equal to a Raman active vibrational mode, no coherent phonons are produced. The three-wave-mixing signal was actually used[8] to maximize the laser spatial overlap at the focal volume inside the crystal. The dependence of the intensity of the three-wave-mixing signal was also determined as a function of the intensity of s-laser with the l-laser again fixed at 135 MW/cm^2. The result is shown in Fig. 2(c).

The results indicated in Figs. 2(a) and 2(b) were repeated for various intensities of the l-laser instead of the s-laser. The results are qualitatively similar, with increases in laser power causing a more rapid decrease in the peak intensities of the vibronic sidebands. Since the l-laser also pumps the luminescence from the bound exciton, an analysis of the results is more complicated than that due to variations in the power of the s-laser alone. We do not, therefore, pursue this point further.

III. THEORETICAL BASIS

In order to understand the results presented above, it becomes necessary to examine the process under which coherent LO phonons are generated. For this purpose we represent the coherent phonon state by a classical, damped harmonic oscillator driven by a force related to CRE of the lattice[9] and to another force related to a concurrent nonlinear polarization of the lattice ions. Hence

$$\mu(\ddot{w}+\Gamma\dot{w}+\omega_{\mathrm{LO}}^2 w)=\hat{1}\cdot\bar{R}\mathbf{E}_l\mathbf{E}_s-\frac{4\pi e^*}{\epsilon_\infty}(\hat{1}\cdot\mathbf{P}_{\mathrm{NL}})\,, \quad (1)$$

In Eq. (1), μ is the reduced lattice mass, w the coherent amplitude, Γ is an *ad hoc* damping rate, $\hat{1}$ a unit polarization vector directed along the LO phonon propagation direction, $\bar{R}$ the Raman tensor associated with LO phonons, $\mathbf{E}_i$ the corresponding laser field intensities at the laser frequency of ω_i, e^* the effective lattice charge, ϵ_∞ the high-frequency dielectric constant, and $\mathbf{P}_{\mathrm{NL}}$ the nonlinear polarization.

Note from Eq. (1) that the coherent LO phonon state can be driven resonantly by both the Raman interaction (if $\omega_l-\omega_s=\omega_{\mathrm{LO}}$) and by the nonlinear polarization $\mathbf{P}_{\mathrm{NL}}$ ($\omega_{\mathrm{LO}}=\omega_l-\omega_s$). We refer to the right-hand side of Eq. (1) as the driving force, F_{LO}. Its evaluation, particularly in the presence of bound and "free" carriers, is rather involved. A synopsis of the derivation appears in Appendix A. Here we write down only the final form, which is

$$F_{\mathrm{LO}}\propto\left[R+\frac{8\pi e^*|\chi^{(2)}|}{\epsilon_\infty}\times\left[1-\frac{24\pi\chi^{(3)}}{0.017}\eta(|\mathbf{E}_l|^2+|\mathbf{E}_s|^2)\right]\right]E_lE_s\,, \quad (2)$$

where we have made the simplification $\chi^{(3)}=\chi^{(3)}_{1111}=\chi^{(3)}_{1122}=\chi^{(3)}_{1221}$ for the elements of the third-order non-

linear electronic susceptibility, and $R=R^{z}_{xy}$ and $|\chi^{(2)}|=|\chi^{(2)}_{xyz}|$. It is clear from Eq. (2) that in the event of high enough values of the laser power, it becomes possible for the term containing $\chi^{(3)}$ to lead to a net decrease in the F_{LO}, which in turn results in a decrease in the production of coherent LO phonons.

We first discuss the results obtained for the dependence of the three-wave-mixing signal at $2\omega_l-\omega_s$ on the incident laser power [see Fig. 2(c)]. From the general theorems of nonlinear mixing,[10] the intensity of this signal

$$I_{3w}(2\omega_l-\omega_s)\propto|\mathbf{P}_{\mathrm{NL}}(2\omega_l-\omega_s)|^2$$
$$\propto|\bar{\chi}^{(3)}\vdots\mathbf{E}_l\mathbf{E}_l\mathbf{E}_s|^2 .$$

Thus with E_l fixed, I_{3w} should increase linearly with the s-laser power, $|E_s|^2$. However, the results of Fig. 2(c) clearly show that the increase is more rapid than linear implying that an additional, power-dependent, contribution to $\chi^{(3)}$ exists. Similarly, from Eq. (1), $|w_{\mathrm{LO,LA}}|^2 \propto |E_l|^2|E_s|^2$ and from the fact that the vibronic sideband intensities, $I_{\mathrm{LO,LA}}$, are also proportional to $|w_{\mathrm{LO,LA}}|^2$, one would expect that the sidebands increase linearly with the power of the s-laser. But, again, the experimental results for the LO and LA sideband depicted in Figs. 2(a) and 2(b) imply that this simple argument is not valid in this case.

IV. ANALYSIS AND DISCUSSION

We propose that the source of the nonlinear power dependence arises from the presence of an electron-hole plasma. Under these circumstances both $\chi^{(2)}$ and $\chi^{(3)}$ possess components associated with bound electrons, $\chi^{(i)}_b$, and with free electrons or those associated with the electron-hole plasma, $\chi^{(i)}_f$. Note that $\chi^{(2)}_f$ vanishes because of time reversal symmetry. Free carriers are generated most likely, in our experiment, through a two-step process illustrated in Fig. 3; the first component of which is the excitation of a bound exciton through absorption of l-laser light, followed by the absorption of either l- or s-photons. The two-phonon process at $2\omega_s$ no doubt also occurs, but must be several orders of magnitude weaker since no observable recombination or zero phonon excitonic luminescence was observed if only the s-laser was used. The most likely initial result is the formation of free carriers in the Γ_{15} conduction band (and a corresponding hole in the valence band)[11] which decay through multistep incoherent LO phonon generation to form, within a time short compared to our observation time,[4] an electron-hole plasma at, e.g., the minimum at the X point of the Γ_1 band. Based on our model of the plasma formation, we consider the following rate equations:

$$\frac{dN^*}{dt}=(N_0-N^*-n_{e\text{-}h})\sigma_0 I_l-N^*(\sigma_l I_l+\sigma_s I_s)-\frac{N^*}{t^*} \tag{3}$$

and

$$\frac{dn_{e\text{-}h}}{dt}=N^*(\sigma_l I_l+\sigma_s I_s)-\frac{n_{e\text{-}h}}{t_c}\approx N^*(\sigma_l I_l+\sigma_s I_s)\,, \tag{4}$$

where N_0, N^*, and $n_{e\text{-}h}$ are, respectively, the concentration of nitrogen impurities, excited bound excitons and photoexcited electron-hole (e-h) carriers; t^* and t_c are, respectively, the lifetime of bound excitons and of e-h carriers; σ_0, σ_l, and σ_s are the cross sections for the excitation of bound excitons, and the excitation of a bound exciton to form a free carrier through a further absorption of either l- or s-laser light; and I_l and I_s are the photon flux of the l- or s-laser light. The last approximation in Eq. (4) was made since our interest is the solution within a time of $t_p=5$ ns (duration of our laser pulse) while the carrier lifetime t_c is about a microsecond.

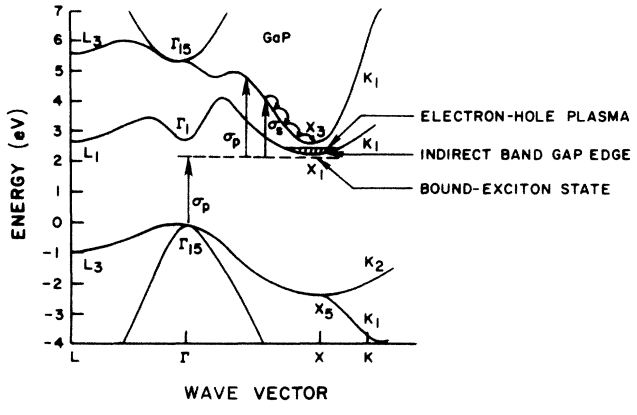

FIG. 3. Band structure of GaP from Ref. 11, with the proposed excitation of the bound exciton indicated by vertical arrows. The probable decay of the free carrier via emission of LO phonons to the minimum at the X_3 level is also indicated, as is the probable location of the electron-hole plasma. Note that the excitation of the bound exciton does not conserve wave vector.

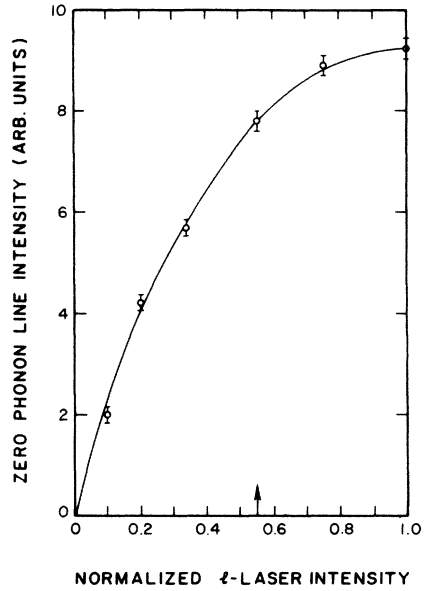

FIG. 4. Change of zero-phonon line intensity as the function of l-laser. The intensity of the l-laser is normalized to 245 MW/cm^2.

When the time dependence of the laser pulse is simplified to a 5-ns duration square pulse, the approximate solutions for N^* and $n_{e\text{-}h}$ can be written as

$$\frac{N^*}{N_0}=\frac{t_p\sigma_0 I_l}{(r_- - r_+)}(e^{-r_+}-e^{-r_-}) \tag{5}$$

and

$$\frac{n_{e\text{-}h}}{N_0}=1+\frac{r_+e^{-r_-}-r_-e^{-r_+}}{r_- - r_+}\ , \tag{6}$$

where $r_-\approx t_p\sigma_0 I_l+t_p/t^*$ and $r_+=t_p(\sigma_l I_l+\sigma_s I_s)$.

We have measured the change of the zero-phonon line luminescence intensity ($\propto N^*$) as a function of the l-laser intensity. The result is shown in Fig. 4. By comparing Eq. (5) under the condition that $I_s=0$ to the experimental result in Fig. 4, we find the best fit values $t_p\sigma_0 I_l^0\simeq 0.88\pm 0.03$ and $t_p\sigma_l I_l^0=0.29\pm 0.02$ when $I_l^0=135$ MW/cm$^2/\hbar\omega_l$ and $t_p/t^*\simeq 0.14$ is used since $t^*\simeq 35$ ns (Ref. 6) at 4.2 K.

Furthermore, from Eq. (5), a linear decrease of N^* is predicted for increasing I_s and fixed I_l^0, i.e.,

$$N^*(\text{fixed } I_l^0, I_s)\simeq\frac{g(e^{-r}-e^{-G})}{(G-r)}\left[1-\left[\frac{e^{-r}}{e^{-r}-e^{-G}}-\frac{1}{G-r}\right]r_s\right],$$

where $g=t_p\sigma_0 I_l^0$, $r=t_p\sigma_l I_l^0$, $G=g+t_p/t^*$, and $r_s=t_p\sigma_s I_s$. An 11% decrease of N^* was observed when the maximum intensity of s-laser ($I_s^0=135$ MW/cm$^2\hbar\omega_s$) was applied together with I_t^0. This implies that

$$\left[\frac{e^{-r}}{e^{-r}-e^{-G}}-\frac{1}{G-r}\right]r\kappa=0.11\ , \tag{7}$$

where $\kappa=\sigma_s/\sigma_l$.

By inserting the numerical values for G and r into Eq. (7), one finds $\kappa=0.66$. Similarly, a linear approximation of Eq. (6) leads to

$$n_{e\text{-}h}\simeq\frac{N_0}{G}(e^{-G}+G-1)r(1+\kappa x)\approx N_h(1+\kappa x)\ , \tag{8}$$

where $N_h=6.4\times 10^{15}$ cm^{-3} and $x=I_s/I_l^0$. This result indicates that $\sim 10^{16}$ cm^{-3} of e-h carriers are excited when $x=1$ under our experimental conditions.

The full expression for $\chi^{(3)}$ under these circumstances is then

$$\chi^{(3)}=\chi_b^{(3)}+\chi_f^{(3)}=\chi_b^{(3)}+Cn_{e\text{-}h} \tag{9}$$

in which C is a material constant which depends mainly on the band nonparabolicity.[12] By substituting Eq. (8) into the expression for $\chi_f^{(3)}$ in Eq. (9), one can express the power dependence of $\chi_f^{(3)}$ as

$$\chi_f^{(3)}=\chi_b^{(3)}h_\chi(1+\kappa x)\ , \tag{10}$$

in which h_χ represents an enhancement factor of $\chi_f^{(3)}$ with respect to $\chi_b^{(3)}$. It follows from Eq. (10) that the dependence of the three-wave-mixing signal on the s-laser intensity can be written as

$$I_{3w}(2\omega_p-\omega_s)\propto(|E_l^0|^2)^3|\chi_b^{(3)}|^2\times[1+h_x(1+\kappa x)]^2 x\ . \tag{11}$$

The dashed curve of Fig. 3(c) was obtained as a best fit of expression (11) to the data points, which yields $h_\chi=5.4\pm 0.45$, such that the enhancement factor due to e-h carriers equals $+8.9\pm 1$ when the s-laser power is at its maximum. We have previously reported[13] $3\chi_b^{(3)}$ to be of the order of 10^{-9} esu.

Hence, by substituting Eq. (10) into (2),

$$F_{\rm LO}\propto\left[1+\frac{8\pi e^*1|\chi^{(2)}|}{\epsilon_\infty R}\{1-0.1[1+h_\chi(1+\kappa x)]\times(1+x)\}\right]E_l^0E_s\ , \tag{12}$$

where

$$\frac{24\pi\chi_b^{(3)}}{0.017}|E_l^0|^2\eta=0.1$$

is used.

In evaluating $|w|^2\propto|F_{\rm LO}|^2$, the effective force was corrected for the presence of the e-h plasma. Even for the maximum $n_{e\text{-}h}=10^{16}$ cm^{-3}, the plasma frequency $\omega_p\propto(n_{e\text{-}h})^{1/2}$ remains small compared to $\omega_{\rm LO}$. In this weak coupling limit, the solution of the relevant coupled equation of motion[14,15] for the amplitude of the coherent phonons in the presence of the plasma leads to

$$|w|^2\propto|F_{\rm LO}|^2/\{1+[\omega_p^2(1-\omega_{\rm TO}^2/\omega_{\rm LO}^2)/\Gamma\omega_{\rm LO}]^2\}=|F_{\rm LO}|^2\Big/\left[1+0.45\left[\frac{1}{\kappa}+x\right]\right]\ . \tag{13}$$

Note that although $\omega_p\ll\omega_{\rm LO}$, $\omega_p^2/\Gamma\omega_{\rm LO}\gg 1$ and $\omega_p^2(1-\omega_{\rm TO}^2/\omega_{\rm LO}^2)/\Gamma\omega_{\rm LO}=1$, since Γ is of the order of 0.2 cm^{-1} at 4.2κ.[1,2] Accordingly, the denominator of Eq. (13) cannot be neglected. In the evaluation of expression (13), several factors were considered. First, since $|w|^2$ can also be found in this way, so can the phonon energy density, and hence the maximum value of the phonon number density, N. We find $N_{\rm LO}\sim 4.4\times 10^{16}$ cm^{-3} when $x=0.6$. When this value is compared to the total density of states available to the LA phonons, $\rho_{\rm LA}\Delta\omega$, into which coherent LO phonons decay, it can be inferred that the maximum occupation probability, $n_{\rm LA}$, is

$$n_{\rm LA}=\frac{N_{\rm LO}}{\rho_{\rm LA}\Delta\omega}\approx\frac{4.4\times 10^{16}}{1.4\times 10^{19}}\sim 3\times 10^{-3}\ll 1\ ,$$

where $\rho_A\Delta\omega$ has been estimated on the basis of the Debye model and $\omega_{\rm LA}=3.8\times 10^{13}$ sec^{-1}, $\Delta\omega\approx\omega_{\rm LA}/200$ and the

LA phonon sound velocity was assumed to be approximately 10^6 cm/sec. Since $n_{LA} \ll 1$, phenomena which have been predicted to occur when $n_{LA} \gtrsim 1$, such as phonon breakdown[16] and optic-acoustic-phonon collective modes[17] are not expected to be a factor here.

Finally, from Eqs. (12) and (13), we find the LO (or LA) vibronic sideband intensity ($\propto N^* \mid w \mid^2$) as the function of the s-laser (with fixed l-laser power) to be

$$I_{LO(LA)} \propto N^*(x) \mid w \mid^2 \propto \frac{(1-0.11x)\{(1+8\pi e^* \mid \chi_b^{(2)} \mid /R\epsilon_\infty)(1-0.1)[1+h\chi(1+\kappa x)(1+x)]\}^2 x}{1+\{0.46(1/\kappa+x)\}^2} .$$

The solid and dotted lines shown in Figs. 2(a) and 2(b) are obtained as best fits to this equation.

It is, of course, possible that even higher-order terms in

$$P_{NL}(\omega_{LO}) = \chi^{(4)}\{ \mid E_l(\omega_l) \mid^2 + \mid E_s(\omega_s) \mid^2 \} E_l E_s ,$$

such as fourth-order terms, may contribute to our results. Unfortunately, little is currently known of the magnitude of higher-order susceptibilities.

Finally, we attempt to estimate the lifetime of LA$(\omega_{LO}/2, \pm q)$ phonons from the observed spectral width of the anti-Stokes vibronic sidebands as shown in Fig. 1. The transform limited spectral width of the LO$(\omega_{LO}, q \sim 0)$ phonon has been shown to be[1] approximately 0.21 cm^{-1} at 5 K, even when the l- and s-laser spectral width exceeds 6 cm^{-1}.[2] Since the LO optical branch is flat near $q=0$, small uncertainties in the l- and s-laser wave vectors, do not lead to a large spread in ω_{LO}. Subsequently the optical phonons decay into half-energy acoustic phonons conserving energy and wave vector in the process. In the absence of energy conservation, one would assume that the spectral width of the acoustic phonons would exceed that of the optical phonons since $d\omega/dq > 0$ for the acoustic phonons. But energy must simultaneously be conserved, and since the LO phonon spectral width is small, we suspect that the observed acoustic-phonon spectral width should also be small. Clearly, a full analysis of the decay process including real dispersion relationships in GaP is required to completely justify this point. In the absence of such an analysis, we simply impose it as an assumption, and look for other possible sources of the observed spectral widths demonstrated in Fig. 1.

The width of the zero-phonon line associated with the luminescence from the bound exciton is measured experimentally under high resolution to be 3 cm^{-1}. The results of Fig. 1 were, as noted above, observed with an (Gaussian) instrumental halfwidth of 9 cm^{-1}. Convolution of the transform limited spectral width of the LO phonons and the instrumental width, accounts for the observed anti-Stokes linewidth of the LO peak which is determined to be 12 ± 1 cm^{-1} by fitting a Gaussian profile to the data. Similarly, we find the halfwidth of the LA anti-Stokes peak to be 15 ± 1 cm^{-1}. Since we have assumed that all other factors are the same for the LO and LA peaks, we speculate that the difference of 3 ± 1.4 cm^{-1} reflects the additional broading of the LA peak due to lifetime effects. If these crude assumptions are correct, we find the LA $(\omega_{LO}/2, \pm q)$ phonon lifetime to be roughly equal to 2 ± 0.9 ps. If, on the other hand, the source of the observed broadening of the LA peak arises from other factors, then we have found only a lower limit to the acoustic phonon lifetime.

In conclusion, we point out that through the combination of the techniques of coherent Raman excitation and vibronic sideband phonon spectroscopy, it has been possible to verify the earlier postulate that coherent LO $(\omega_{LO}, q \sim 0)$ phonons dephase in GaP through decay into LA $(\omega_{LO}/2, \pm q)$ phonons, that nonlinear polarization must be taken into account and, particularly, that an electron-hole plasma, when present, can strongly influence excitation of coherent phonons.

APPENDIX A

From Eq. (1) the force driving the coherent amplitude, w, is

$$F_{LO} = \hat{1} \cdot \bar{R} \mathbf{E}_l \mathbf{E}_s - \frac{4\pi e^*}{\epsilon_\infty} (\hat{1} \cdot \mathbf{P}_{NL}) . \tag{A1}$$

The Raman term in Eq. (A1) can be evaluated[8] for GaP taking into account the polarization of the dye lasers and the symmetry properties of $\bar{R}$. One finds

$$\hat{1} \cdot \bar{R} \mathbf{E}_l \mathbf{E}_s = 0.66 R E_l E_s \eta , \tag{A2}$$

in which R is the Raman tensor element, E_i the corresponding laser field maximum amplitude and the numerical value 0.66 and $\eta = \frac{4}{5}$ were obtained by the projection of the polarization of l and s lasers with respect to the crystal axes.

Next, since any nonlinear polarization in the crystal at the mixing frequency ω_{LO} can resonantly drive coherent LO phonons, i.e., affect the value of w, it becomes important to consider all possible nonlinear polarization with frequency ω_{LO} induced under the present experimental conditions. The simplest form is

$$\mathbf{P}_{NL}(\omega_{LO} = \omega_l - \omega_s) = \bar{\chi}^{(2)} \cdot \mathbf{E}_l \mathbf{E}_s . \tag{A3}$$

By substituting the polarization vectors for the l- and s-lasers, using the properties of $\chi^{(2)} = \chi^{(2)}_{xyz} = \chi^{(2)}_{zxy} = \chi^{(2)}_{yzx}$ as the only nonvanishing components of the second-order nonlinear susceptibility, one finds[8] that

$$\hat{1} \cdot \mathbf{P}_{NL}(\omega_{LO}) = 0.66(2\chi^{(2)}) \eta E_l E_s ,$$

where the factor of 2 represents the permutation symmetry between the l- and s-lasers.

The term of next-higher order involves a two-step process in which the l- and s-lasers induce a third-order nonlinear polarization at the frequency $2\omega_l - \omega_s$ which, in turn, induces a transverse electrical field at the same fre-

quency.[18] This field interacts again with the laser field $\mathbf{E}_l$ resulting in a nonlinear polarization at $\omega_{\rm LO}$. The pertinent stages are

$$\mathbf{P}_{\rm NL}(2\omega_l-\omega_s)=\bar{\chi}^{(3)}:\mathbf{E}_l\mathbf{E}_l\mathbf{E}_s \ , \tag{A4}$$

which induces

$$\mathbf{E}_I(2\omega_l-\omega_s)=\frac{4\pi\hat{N}[\hat{N}\cdot\mathbf{P}_{\rm NL}(2\omega_l-\omega_s)]}{\Delta\epsilon} \ , \tag{A5}$$

and, finally,

$$\mathbf{P}'_{\rm NL}(\omega_{\rm LO}=\omega_l-\omega_s)=\bar{\chi}^{(2)}\mathbf{E}_I(2\omega_l-\omega_s)\mathbf{E}_l(-\omega_s) \ .$$

Here $\hat{N}$ is a unit vector normal to $\mathbf{k}_N=2\mathbf{k}_l-\mathbf{k}_s$ (the wave vector of the laser field) and

$$\Delta\epsilon=[(c/\omega)^2\mathbf{k}_N\cdot\mathbf{k}_N-\epsilon(\omega)]\approx-0.017 \tag{A6}$$

in which c is the speed of light, $\omega=2\omega_l-\omega_s$, and $\epsilon(\omega)$ is the dielectric constant at ω.

Evaluation of the $\hat{I}$ component of $\mathbf{P}'_{\rm NL}(\omega_{\rm LO})$ is straightforward though tedious. The result is

$$\hat{1}\cdot\mathbf{P}'_{\rm NL}(\omega_{\rm LO})=-0.66\chi^{(2)}\eta^2C_\chi 3\chi^{(3)}\,|\,E_l\,|^2E_lE_s \ , \tag{A7}$$

where $C_\chi=8\pi/0.017$, and the simplification $\chi^{(3)}\approx\chi_{1111}\approx\chi_{1122}\approx\chi_{1221}$ has been made. The simplification has been shown to be appropriate for the third-order susceptibility due to bound electrons, $\chi_b^{(3)}$, in GaP.[13] The validity of this assumption in the general case, i.e., when the contribution to $\chi^{(3)}$ from free electrons or from an electron-hole plasma, $\chi_f^{(3)}$ is also present, has not as yet been explored. Nevertheless, the same assumption is applied to $\chi_f^{(3)}$, since we believe that it is enough to obtain at least a qualitative understanding of the experimental results presented here.

There is one more contribution to $\mathbf{P}_{\rm NL}(\omega_{\rm LO})$ due to a different two-step process. Note that another third-order polarization,

$$\mathbf{P}_{\rm NL}(2\omega_s-\omega_l)=\bar{\chi}^{(3)}:\mathbf{E}_l\mathbf{E}_s\mathbf{E}_s \ ,$$

induces $\mathbf{E}_I(\omega_s-\omega_l)$ at a frequency $(2\omega_s-\omega_l)$ such that

$$\mathbf{P}''_{\rm NL}(\omega_{\rm LO})=\bar{\chi}^{(2)}\cdot\mathbf{E}_I(-2\omega_s+\omega_l)\mathbf{E}_s(\omega_s) \ . \tag{A8}$$

In a manner similar to that applied to derive Eqs. (A4)–(A7), we find another contribution to the polarization such that

$$\hat{1}\cdot\hat{P}''_{\rm NL}(\omega_{\rm LO})=-0.66(2\chi^{(2)})\eta^2C_\chi 3\chi^{(3)}\,|\,E_s\,|^2E_lE_s \ . \tag{A9}$$

Finally, by substituting the results of (A2), (A7), and (A9) into (A1) we obtain

$$F_{\rm LO}=0.66\eta\left[R-\frac{8\pi e^*\chi^{(2)}}{\epsilon_\infty}[-C_\chi 3\chi^{(3)}(\,|\,E_l\,|^2+\,|\,E_s\,|^2)\eta]\right]E_lE_s \ . \tag{A10}$$

In the absence of free carriers, Eq. (A10) becomes

$$F_{\rm LO}=0.66\eta\left[R+\frac{4\pi e^*}{\epsilon_\infty}\chi^{(2)}_{\rm eff}\right]E_lE_s \ , \tag{A11}$$

where

$$\chi^{(2)}_{\rm eff}=\,|\,2\chi_b^{(2)}\,|\,[1-C_\chi 3\chi_b^{(3)}(E_l^2+E_s^2)\eta] \ . \tag{A12}$$

Here, the sign of R is changed due to the fact that R and $\chi_b^{(2)}$ have opposite signs.[19] Experimentally we find[8] that $|\,E_l\,|^2=10^{15}$ esu when the l-laser power is fixed at 135 MW/cm^2, $\eta\approx\frac{4}{5}$ and $3\chi^{(3)}=8\times10^{-10}$ esu.[12,13] The second term in (A12) can be written as

$$H(x)=C_\chi 3\chi_b^{(3)}\eta\,|\,E_l\,|^2(1+x)\approx0.1(1+x) \ ,$$

where $x=|\,E_s\,|^2/|\,E_l\,|^2$. Since the power of the s-laser can be varied up to a limit of 135 MW/cm^2, i.e., up to the fixed value of the l-laser, $x<1$. Thus $H(x)<0.2\ll1$. Thus the higher order contributions to $\chi^{(2)}_{\rm eff}$ can be neglected in the absence of free carriers.

ACKNOWLEDGMENTS

Financial support for this research has been obtained through the U.S. Army Research Office (Durham, NC) Grant No. DAAG29-83-K-0091.

*Present address: Optical Sciences Center, The University of Arixona, Tucson, AR 85721.

†Present address: Department of Physics, University of California at Irvine, Irvine, CA 92717.

[1]J. Kuhl and W. E. Bron, Solid State Commun. **49**, 935 (1984).

[2]W. E. Bron, J. Kuhl and B. K. Rhee, Phys. Rev. B **34**, 6961 (1986).

[3]This need not always be so. For example, $\mathbf{q}\sim0$ TO phonons in GaP have been postulated to decay to a continuum of states near the X point. [See A. S. Barker, Phys. Rev. **165**, 917 (1968)]. Similarly, we report in Ref. 2 that this is not the case for ZnSe.

[4]See J. A. Kash, J. C. Tzang, and J. M. Hvam, Phys. Rev. Lett. **19**, 2151 (1985) and references cited therein.

[5]W. E. Bron and W. Grill, Phys. Rev. B **16**, 5303 (1977); **16**, 5315 (1977); T. E. Wilson, F. M. Lurie, and W. E. Bron, *ibid.* **30**, 6103 (1984).

[6]D. G. Thomas, M. Gershenson, and J. J. Hopfield, Phys. Rev. **131**, 2347 (1963); D. G. Tomas and J. J. Hopfield, *ibid.* **150**, 580 (1966).

[7]C. Hanna, P. A. Kaerkkaeiner, and R. Wyatt, Opt. and Quant. Elect. **7**, 115 (1975)

[8]B. K. Rhee, Ph.D. thesis, Indiana University, 1985 (unpublished).

[9]E. Garmire, F. Panderese, and C. H. Townes, Phys. Rev. Lett. **11**, 160 (1963).

[10]N. Bloembergen, *Nonlinear Optics* (Benjamin, New York, 1965).

[11]M. L. Cohen and T. K. Bergstrasser, Phys. Rev. **141**, 789 (1966).

[12]S. S. Jha and N. Bloembergen, Phys. Rev. **171**, 891 (1968).

[13]B. K. Rhee, W. E. Bron, and J. Kuhl, Phys. Rev. B **30**, 7358 (1984).

[14]J. E. Kardontchik and E. Cohen, Phys. Rev. Lett. **42**, 669 (1979).

[15]See, e.g., A. Mooradian, in *Laser Handbook,* edited by F. T. Arecchi and E. O. Schultz-DuBois (North Holland, Amsterdam, 1972), Vol. II, p. 1309.

[16]R. Orbach, Phys. Rev. Lett. **16**, 15 (1966), see also R. Orbach, IEEE Trans. Sonics Ultrason. **SU-14**, 140 (1967).

[17]S. A. Bulgadeev and I. B. Levinson, Zh. Eksp. Teor. Fiz. **67**, 2341 (1974) [Sov. Phys.—JETP **40**, 1161 (1975)] and references cited therein.

[18]C. Flytzanis and N. Bloembergn, Prog. Quant. Electr. **4**, 271 (1976).

[19]W. L. Faust and C. H. Henry, Phys. Rev. Lett. **17**, 1265 (1966).